Lawrence Berkeley National Laboratory
LBL Publications

Title

Skew Harmonics Suppression in Electromagnets with Application to the Advanced Ligh Source (ALS) Storage Ring Corrector Magnet Design

Permalink

https://escholarship.org/uc/item/8ws4z6zh

Authors

Schlueter, R.D.
Halbach, K.

Publication Date

1993-09-01

eScholarship.org Powered by the California Digital Library
University of California

LBL-34660
UC-410

Lawrence Berkeley Laboratory
UNIVERSITY OF CALIFORNIA

Accelerator & Fusion Research Division

Presented at the Thirteen International Conference on Magnet Technology, Victoria, B.C., Canada, September 20–24, 1993, and to be published in the Proceedings

Skew Harmonics Suppression in Electromagnets with Application to the Advanced Light Source (ALS) Storage Ring Corrector Magnet Design

R. Schlueter and K. Halbach

September 1993

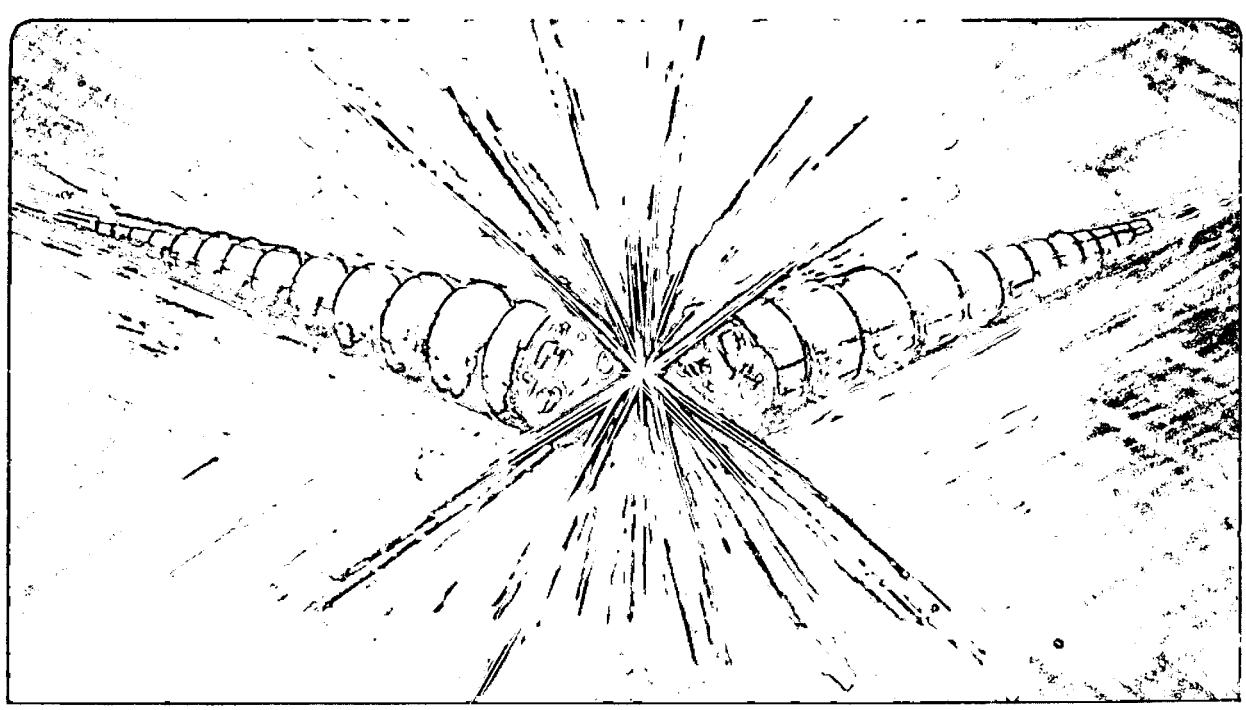

Prepared for the U.S. Department of Energy under Contract Number DE-AC03-76SF00098

REFERENCE COPY
Does Not
Circulate
Bldg. 50 Library.
Copy 1
LBL-34660

DISCLAIMER

This document was prepared as an account of work sponsored by the United States Government. While this document is believed to contain correct information, neither the United States Government nor any agency thereof, nor the Regents of the University of California, nor any of their employees, makes any warranty, express or implied, or assumes any legal responsibility for the accuracy, completeness, or usefulness of any information, apparatus, product, or process disclosed, or represents that its use would not infringe privately owned rights. Reference herein to any specific commercial product, process, or service by its trade name, trademark, manufacturer, or otherwise, does not necessarily constitute or imply its endorsement, recommendation, or favoring by the United States Government or any agency thereof, or the Regents of the University of California. The views and opinions of authors expressed herein do not necessarily state or reflect those of the United States Government or any agency thereof or the Regents of the University of California.

LBL-34660

Skew Harmonics Suppression in Electromagnets with Application to the Advanced Light Source (ALS) Storage Ring Corrector Magnet Design*

R. Schlueter and K. Halbach

Advanced Light Source
Accelerator and Fusion Research Division
Lawrence Berkeley Laboratory
University of California
Berkeley, CA 94720

September 1993

Paper presented at the 13th International Conference on Magnet Technology
Victoria, B.C., Canada
September 20-24, 1993

*This work was supported by the Director, Office of Energy Research, Office of Basic Energy Sciences, Materials Sciences Division of the U.S. Department of Energy, under Contract No. DE-AC03-76SF00098.

Skew Harmonics Suppression in Electromagnets with Application to the Advanced Light Source (ALS) Storage Ring Corrector Magnet Design

R.D. Schlueter and K. Halbach
Lawrence Berkeley Laboratory, Berkeley, California 94720

Abstract- **An analytical expression for prediction of skew harmonics in an iron core combined function regular/skew dipole magnet due to arbitrarily positioned electromagnet coils is developed. A structured approach is presented for the suppression of an arbitrary number of harmonic components to arbitrarily low values. Application of the analytical harmonic strength calculations coupled to the structured harmonic suppression approach is presented in the context of the design of the ALS storage ring corrector magnets, where quadrupole, sextupole, and octupole skew harmonics were reduced to less than 1.0% of the skew dipole at the beam aperture radius $r = 3.0$ cm.**

I. INTRODUCTION

Harmonics suppression, required in many accelerator physics magnet applications, is usually performed by shimming an iron dominated magnet. Conductor dominated magnets necessitate a different approach. Such is the case for the ALS combined function regular/skew dipole corrector magnets. The effect of field errors in the ALS storage ring on the electron beam's dynamic aperature has been analyzed [1] and harmonics suppression requirements for these magnets have been tabulated [2]: skew quadrupole (sQ), sextupole (sS), and octupole (sO) components at $|r| = 3.0$ cm are not to exceed 1.4%, 1.0%, and 1.4%, respectively, of the skew dipole (sD).

II. ANALYTICAL EXPRESSIONS FOR SKEW HARMONIC COMPONENTS

Fig. 1a shows the gap portion of a wide [x-direction] electromagnet with current filaments of magnitude $\pm I$ at z_0 and z_0^*, respectively, giving rise to a skew [x-direction] dipole. The return paths for the currents on the outsides of the iron yoke are not shown. The width [x-direction] of the iron pole face yoke is assumed effectively infinite in the analytical model. Exponential decay of field errors as one moves towards the origin from the corner of the iron pole insures that this approximation will not result in large errors of calculated harmonic components near the location of the beam axis (the origin in Fig. 1a).

Manuscript received September 20, 1993. This work was supported by the Director, Office of Energy Research, Office of Basic Energy Sciences, Material Sciences Div., of the U.S. Dept. of Energy under Contract No. DE-AC03-76SF00098.

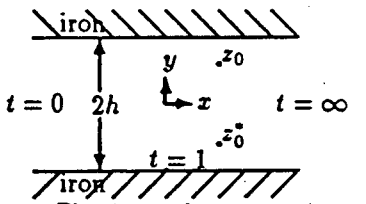

Fig. 1a. z plane (electromagnet skew dipole geometry).

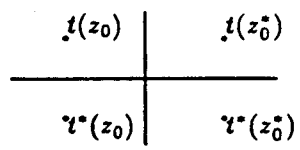

Fig. 1b. t plane (Schwarz-Christoffel transformed geometry).

We shall use a Schwarz-Christoffel transformation to conformally map the gap region between $z = (x, \pm h)$ of Fig. 1a to the upper half t plane shown in Fig. 1b. Choosing $t = \infty$ at $z = +\infty$ results in the transformation $\frac{dz}{dt} = \frac{1/k}{t-a}$. Choosing $t = a = 0$ at $z = -\infty$ makes $\frac{1}{k}$ take on the value $\frac{2h}{\pi}$ since at $t = 0$, $Im(\Delta z) = Im(\oint_{t=0} \frac{1}{kt} dt), \Longrightarrow 2h = Im(\frac{\pi i}{k}) = \frac{\pi}{k}$. Integrating with respect to t gives $z = \frac{2h}{\pi} \ln t + c, \Longrightarrow t = e^{\frac{\pi(z-c)}{2h}}$. Choosing $t = 1$ at $z = -ih$ makes c take on the value $-ih$. The complete $t \rightleftharpoons z$ transformation is thus

$$z = \frac{2h}{\pi} \ln t - ih, \Longrightarrow t = ie^{\frac{\pi z}{2h}} = ie^{kz} = ie^{\alpha}, \qquad (1)$$

where $k \equiv \frac{\pi}{2h}$ and $\alpha \equiv kz$.

For the filament of magnitude $+I$ at z_0 and its image in the t plane about the real axis, which makes the magnetic field perpendicular to the air-iron interface, the complex magnetic potential $F(t) \equiv A + iV$ (where $\nabla \times A = H$, $\nabla V = -H$) is given by $F(t) = \frac{-I}{2\pi} \ln(t - t(z_0))(t - t^*(z_0))$.

The magnetic field is related to the complex potential by $H^*(z) = i\frac{dF}{dz}$. For this case we have

$$H^*(z) = i\frac{dF/dt}{dz/dt} = \frac{Ike^{\alpha}}{2\pi i}\left[\frac{1}{e^{\alpha} - e^{\alpha_0}} + \frac{1}{e^{\alpha} + e^{\alpha_0^*}}\right]. \qquad (2)$$

For current filaments of magnitude $\pm I$ at z_0 and z_0^*, respectively, and their images in the t plane about the real axis, we have for $\hat{H}^*(z) \equiv H^*(z)/\frac{Ik}{2\pi i}$:

$$\hat{H}^*(z) = \frac{e^{\alpha}}{e^{\alpha} - e^{\alpha_0}} + \frac{e^{\alpha}}{e^{\alpha} + e^{\alpha_0^*}} + \frac{-e^{\alpha}}{e^{\alpha} - e^{\alpha_0^*}} + \frac{-e^{\alpha}}{e^{\alpha} + e^{\alpha_0}}$$
$$= \frac{1}{Sinh(\alpha - \alpha_0)} - \frac{1}{Sinh(\alpha - \alpha_0^*)}, \qquad (3)$$

where the relations $t(z_0) = ie^{\alpha_0}$, $t(z_0^*) = ie^{\alpha_0^*}$, $t^*(z_0) = -ie^{\alpha_0^*}$, and $t^*(z_0^*) = -ie^{\alpha_0}$ have been used.

For a pair of current sheets of magnitude $\pm I'$ from z_1 to z_2 and from z_1^* to z_2^*, respectively, and their images in the t plane about the real axis, we have for $\tilde{H}^*(z) \equiv H^*(z)/\frac{I'}{2\pi i}$ by integrating the terms in (3) with respect to z_0 or z_0^*, as appropriate:

$$\tilde{H}^*(z) = \ln\left(\frac{e^{\alpha_0^*-\alpha}-1}{e^{\alpha_0^*-\alpha}+1}\right)\Bigg|_{\alpha_1^*}^{\alpha_2^*} - \ln\left(\frac{e^{\alpha_0-\alpha}-1}{e^{\alpha_0-\alpha}+1}\right)\Bigg|_{\alpha_1}^{\alpha_2}. \quad (4)$$

We now decompose these expressions for $H^*(z)$ into harmonic components. Define $G(z) \equiv \frac{1}{Sinh(z)}$. Then,

$$G(\alpha-\alpha_0) = \frac{1}{Sinh(\alpha-\alpha_0)} = \Sigma_0 \alpha^n a_n \quad (5)$$

$$where \quad n!a_n = \frac{\partial^n}{\partial\alpha^n}\left(\frac{1}{Sinh(\alpha-\alpha_0)}\right)\Bigg|_{\alpha=0} =$$

$$(-1)^{n+1}\frac{\partial^n}{\partial\alpha_0^n}\left(\frac{1}{Sinh(\alpha_0)}\right) = (-1)^{n+1}G^n(\alpha_0) \quad (6)$$

and where the first equality in (6) is true for any function $f(\alpha-\alpha_0)$ that can be expanded in the power series $\Sigma_0\alpha^n a_n$, the second equality in (6) is true whenever $f(\alpha-\alpha_0)$ is an odd function, and where the exponent n in $G^n(\alpha_0)$ refers to differentiation with respect to α_0.

Therefore,

$$G(\alpha-\alpha_0) - G(\alpha-\alpha_0^*) = \Sigma_0\alpha^n(a_n - c_n)$$
$$= \Sigma_0\frac{\alpha^n}{n!}(-1)^{n+1}\left\{\frac{\partial^n G(\alpha_0)}{\partial\alpha_0^n} - \frac{\partial^n G(\alpha_0^*)}{\partial\alpha_0^{*n}}\right\}$$
$$= \Sigma_0\frac{\alpha^n}{n!}(-1)^{n+1}\left\{2iIm\left[\frac{\partial^n G(\alpha_0)}{\partial\alpha_0^n}\right]\right\}. \quad (7)$$

Thus, the multipole components for a pair of current filaments of magnitude $\pm I$ at z_0 and z_0^*, respectively, are given by

$$H^*(z) = \frac{Ik}{\pi}\Sigma_0\frac{\alpha^n}{n!}(-1)^{n+1}Im\left[\frac{\partial^n}{\partial\alpha_0^n}\left(\frac{1}{Sinh(\alpha_0)}\right)\right]$$
$$= \frac{Ik}{\pi}Im\left\{-\frac{1}{S} + \alpha\frac{-C}{S^2} - \frac{\alpha^2}{2}\left(\frac{1}{S}+\frac{2}{S^3}\right)\right.$$
$$\left. + \frac{\alpha^3}{6}(-C)\left(\frac{1}{S^2}+\frac{6}{S^4}\right) + \ldots\right\} \quad (8)$$

where $S \equiv Sinh(\alpha_0)$ and $C \equiv Cosh(\alpha_0)$.

For a pair of current sheets of magnitude $\pm I'$ from z_1 to z_2 and from z_1^* to z_2^*, respectively, the multipole components are given by

$$H^*(z) = \frac{I'}{\pi}\Sigma_0\alpha^n Im(kb_n), \quad (9)$$

where $\alpha \equiv kz = \frac{\pi z}{2h}$ and

$$kb_0 = -\int_{\alpha_1}^{\alpha_2}\frac{1}{Sinh(\alpha_0)}d\alpha_0 = -\ln\left(\frac{e^{\alpha_0}-1}{e^{\alpha_0}+1}\right)\Bigg|_{\alpha_1}^{\alpha_2},$$

$$kb_n = \frac{(-1)^{n+1}}{n!}\frac{\partial^{n-1}}{\partial\alpha_0^{n-1}}\left(\frac{1}{Sinh(\alpha_0)}\right)\Bigg|_{\alpha_1}^{\alpha_2}, n \geq 1. \quad (10)$$

III. ELECTROMAGNET COIL DESIGN

A. Design methodology: How to go about a design.

Judicious selection of coil positions can effectively reduce unwanted skew harmonics. An experimental trial and error coil positioning approach may be feasible for the elimination of one or two harmonics, but for suppression of several harmonics, this procedure is fatally flawed in that it may never converge to a desired solution. This scenario can arise because changes in harmonic component strengths are not even monotonic, much less linear, with coil position. Here, a structured approach to harmonic suppression is described.

We use as an example the geometry and specifications for the ALS storage ring corrector magnets (Fig. 2), where it is desired to reduce to arbitrarily small values the sQ, sS, and sO components; a coil arrangement consisting of three independently positionable (in x) coil packets is employed. (Coils giving rise to the regular y-direction field are not shown.)

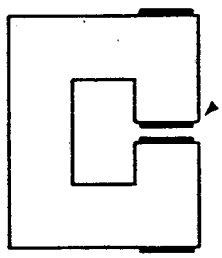

Fig.2a. C-magnet.

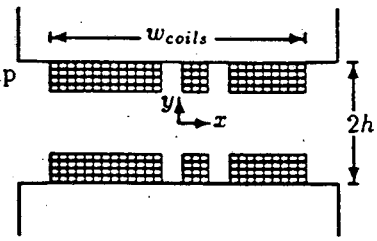

Fig 2b. Blow-up of gap region.

Ignoring 3-D fringe field effects, the finite pole face width, and the C-shape induced asymmetry, (9) may be used to predict harmonic strength dependencies on coil position for packets of various widths (Fig. 3).

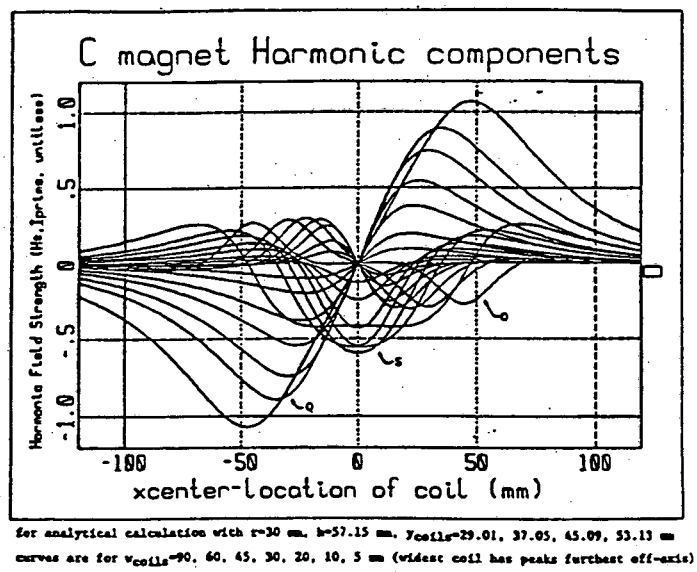

for analytical calculation with r=30 mm, h=57.15 mm, y_{coils}=29.01, 37.05, 45.09, 53.13 mm
curves are for w_{coils}=90, 60, 45, 30, 20, 10, 5 mm (widest coil has peaks furthest off-axis)

Fig. 3. Skew harmonics strength dependence on coil position (analytical).

A base arrangement of coil packets is selected, from which harmonics may be calculated according to (9) by superposing contributions from each packet at its respective location. Let $x_{i_{base}}$ = the base x-coordinate of the center of packet i, for $i = 1,2,3$. An ixj = 3x3 matrix M calculated from $\frac{\partial}{\partial x}$ of (9) relates changes in position of the i packets to changes in the j-length solution vector $\vec{H}^*$ consisting of sQ, sS, and sO:

$$\vec{H}^* = M\Delta\vec{x} + \vec{H}^*_{base} \tag{11}$$

where $\vec{H}^*_{base}$ is comprised of sQ, sS, and sO harmonic strengths when coil packets are at their base positions and $\Delta\vec{x}$ are perturbations of packets from those positions.

A [hopefully improved] guess at a desired coil arrangement is found from inverting the matrix:

$$\vec{x}_{new} = \vec{x}_{base} + \Delta\vec{x},\ \Delta\vec{x} = M^{-1}(\vec{H}^*_{desired} - \vec{H}^*_{base}). \tag{12}$$

Nonlinearities over coil packet position perturbations $\Delta\vec{x}$ necessitate iteration. Several points worth noting:

- The $\vec{x}_{new}$ may move toward a local maximum, in which case a converged solution may not be possible for the chosen $\vec{x}_{base}$. The curves in Fig. 3 will indicate this.
- There may be no solution possible for a chosen set of coil packet widths regardless of $\vec{x}_{base}$. A set of widths for which a solution does exist can be selected using Fig. 3.
- Operating near a local maximum is to be avoided only if one is depending on the perturbation of that particular packet to significantly change that particular harmonic.
- One must insure that matrix element variations over packet excursions from base positions will not cause M to become singular, and thus the problem, intractable. Experimental uncertainties and the effect of matrix element variations on the condition of M are discussed in [3].
- Higher order harmonics may also be nulled following the techniques described herein [3].

B. ALS Storage Ring Corrector Magnets

1. Coil Design

Experimental results of harmonics strength dependence on ALS corrector magnet coil packet position for packets of various widths compared with its 2-D analytical counterpart confirmed that (9) models the observed harmonics behavior very well. This is true because field errors decay exponentially as one moves inside the magnet from the corners of the iron poles. Minor differences are attributable to 3-D fringe fields and to C-shape asymmetry, which has the effect of making the magnitudes of experimentally measured positive and negative peaks of the sQ vs. x plot (cf. Fig. 3) differ by $\sim$ 16%.

The coil design outline follows:

- The 24 turns of width 7.85 mm/turn in each of four layers make total wound coil width 188.4 mm, leaving 31mm of play for coil positioning within the 220 mm mold gap.
- Three indpendently positionable coil packets provide the degrees of freedom to null sQ, sS, and sO.
- To null sQ, the 24 coils were inititially split 13/11, rather than positioning equally-split coils far off-center and suffering a decrease of the fundamental's magnitude.
- For the base arrangement, the 24 coils were further split into three packets 13/3/8, centered at x = -55.0 mm, 23.6 mm, and 66.8 mm. Experimentally obtained sQ, sS, and sO were +1.6%, -1.5%, and -1.0%, respectively.

Additionally, this base position features a well-conditioned matrix M whose elements have units of '$\frac{H^*}{I_r}$/mm packet displacement from base position':

$$M = \begin{pmatrix} -0.005 & 0.006 & -0.0075 \\ 0.013 & -0.014 & 0.0002 \\ -0.007 & -0.009 & -0.0004 \end{pmatrix}. \tag{13}$$

Units of M can be converted to '% sD/mm packet displacement from base position', using the normalized skew dipole strength of '4.0'. Packets #2 and #3 abut in this base position. However, sQ is positive (by design), so iterations drive the 3rd packet in the positive direction from its base position to null sQ. Simultaneous change in sS is minimal since $M_{3,2}$ is small. Since $M_{2,2}$ is large, a smaller positional perturbation of the 2nd packet nulls sS, without overlapping the physical space occupied by the 3rd packet.

- Packet base positions and experimentally obtained values for sQ, sS, and sO are input into a matrix solver code which inverts M and performs the operations given by (11) to give a predicted positioning of the packets which will null sQ, sS, and sO.
- The output configuration is experimentally tested and the three componets are brought to $\leq$ 0.25% of the fundamental in just two iterations. The final configuration comprises packets centered at -56.6 mm, 18.6 mm, and 71.9 mm, yielding experimentally obtained values for sQ, sS, and sO of -0.02%, -0.13%, and -0.10%, respectively.
- Corrector magnets do not operate in isolated environments; nearby iron structures slightly affect skew harmonics. A final, single corrector magnet design was chosen to accomodate the various anticipated environments.

2. Tolerances

x-, y-, and Z-positioning Displacements. The effect of a millimeter x-displacement of a given coil packet on sQ, sS, and sO is given by appropriate elements of M in (13) or alternatively, is calculable using (9). Likewise, the effect of a coil stack-up displacement in the y direction on sQ, sS, and sO is calculable using (9). Experiments of coil packet Z-position displacements with respect to the iron core showed virtually no effect on harmonics over the range of coil movement possible $\pm$ 0.127 cm (0.050").

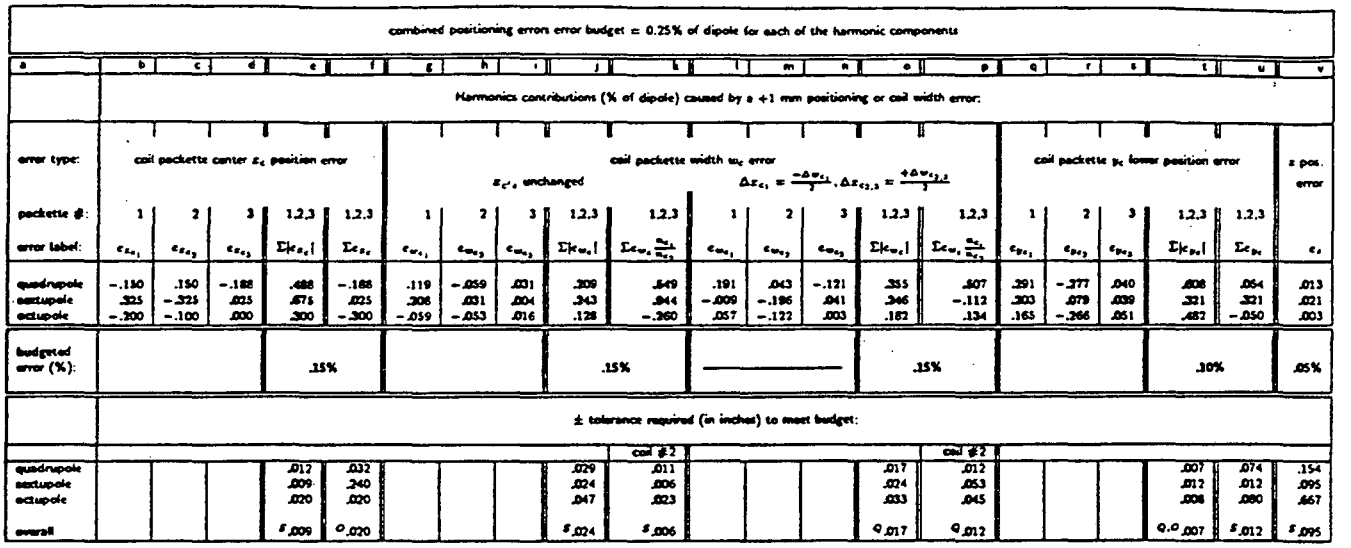

combined positioning errors error budget = 0.25% of dipole for each of the harmonic components

a	b	c	d	e	f	g	h	i	j	k	l	m	n	o	p	q	r	s	t	u	v
Harmonics contributions (% of dipole) caused by a +1 mm positioning or coil width error:																					
error type:	coil packette center x_c position error					coil packette width w_c error, $x_{c'}$ unchanged					coil packette width w_c error, $\Delta x_{c_1} = \frac{-\Delta w_{c_1}}{2}, \Delta x_{c_{2,3}} = \frac{+\Delta w_{c_{2,3}}}{2}$						coil packette y_c lower position error					z pos. error
packette #:	1	2	3	1,2,3	1,2,3	1	2	3	1,2,3	1,2,3	1	2	3	1,2,3	1,2,3	1	2	3	1,2,3	1,2,3	
error label:	$e_{x_{c_1}}$	$e_{x_{c_2}}$	$e_{x_{c_3}}$	$\Sigma\|e_{x_c}\|$	Σe_{x_c}	$e_{w_{c_1}}$	$e_{w_{c_2}}$	$e_{w_{c_3}}$	$\Sigma\|e_{w_c}\|$	$\Sigma e_{w_c}\frac{n_{c_i}}{n_{c_1}}$	$e_{w_{c_1}}$	$e_{w_{c_2}}$	$e_{w_{c_3}}$	$\Sigma\|e_{w_c}\|$	$\Sigma e_{w_c}\frac{n_{c_i}}{n_{c_1}}$	$e_{y_{c_1}}$	$e_{y_{c_2}}$	$e_{y_{c_3}}$	$\Sigma\|e_{y_c}\|$	Σe_{y_c}	e_z
quadrupole	-.150	.150	-.188	.488	-.188	.119	-.059	.031	.209	.549	.191	.043	-.121	.355	.507	.291	-.377	.040	.808	.054	.013
sextupole	.325	-.325	.025	.675	.025	.206	.031	.004	.343	.944	-.009	-.196	.041	.346	-.112	.303	.079	.039	.321	.321	.021
octupole	-.200	-.100	.000	.300	-.300	-.059	-.053	.016	.128	-.260	.057	-.122	.003	.182	.134	.165	-.266	.051	.482	-.050	.003
budgeted error (%):				.15%					.15%					.15%					.10%		.05%
± tolerance required (in inches) to meet budget:																					
										coil #2					coil #2						
quadrupole				.012	.032				.029	.011				.017	.012				.007	.074	.154
sextupole				.009	.240				.024	.006				.024	.053				.012	.012	.095
octupole				.020	.020				.047	.023				.033	.045				.008	.080	.667
overall				s .009	o .020				s .024	s .006				o .017	o .012				$o.o$ .007	s .012	s .095

Fig. 4. Positioning error budget and design tolerances.

Tolerancing Implications. In Fig. 4 harmonics from +1 mm x, y, and Z positioning errors and coil width errors are tabulated. The total positioning errors budget (0.25% of sD for each harmonic) is allocated to distribute the mechanical assembly difficulty uniformly. Tolerances required to meet the error budget for each harmonic are tabulated. For the coil packet width error, two scenarios are investigated: registering from packet centers $x_{c'}$s and from packet inside edges. The latter approach is desired, as sQ rather than sS sets a relaxed packet width tolerance. Important error figures and suggested tolerances are found in columns e, p, u, and v for x_c, w_c, y_c and Z_c, respectively. The sS-limited packet x_c position tolerance of .009" (column e) assumes x_c positionings of the three coil packets are independent. The sQ-limited allowable coil width w_c variation of .012" (column p) for the second coil packet (having three turns) assumes packet widths will be proportionately at variance from the ideal and that the design approach fixing inner x-positions of packets is employed. Tolerances on w_c for the two larger coil packets scales proportionately with their respective x-direction widths. The sS-limited allowable coil y_c position variation of .012" (column u) assumes that the three coil packets' y_c positions will be uniformly at variance from the ideal. Harmonics introduced by Z_c position errors (column v) are insignificant.

Rotating Coil Measurement System Alignment. On-axis harmonics a_n given by $H^*(z) = \Sigma_{n=0} a_n z^n$ are suppressed below 1% of a_0 for $n \leq 3$ as measured by a rotating coil which defines the on-axis position. If subsequently, the coil is off-axis by Δ_z, where $w = z - \Delta_z$, then measured coefficients b_n defined by $H^*(w) = \Sigma_{n=0} b_n w^n$ can be related to the a_n by expanding $H^*(z)$ in w:

(normalized skew dipole strength = 4.0)

$$H^*(z) = \Sigma_{n=0} a_n z^n = \Sigma_{n=0} a_n (w + \Delta_z)^n =$$
$$\Sigma_{n=0} \left\{ w^n \Sigma_{m=n} \left(\frac{a_m m! \Delta_z^{m-n}}{(m-n)!n!} \right) \right\} \equiv \Sigma_{n=0} w^n b_n \quad (14)$$

The $b_{n'}$s can be thought of as measured values of the $a_{n'}$s in error due to the Δ_z coil misalignment. We budget for a coil misalignment-induced error for the n^{th} harmonic of f_n% of a_0 at $|r| = 3$ cm. Defining $\epsilon \equiv \frac{\Delta_z}{r}$ and $p_n \equiv \frac{a_n r^n}{a_0}$, we have

$$f_n \geq \frac{r^n}{a_0} |b_n - a_n| = \frac{r^n}{a_0} \Sigma_{m=n+1} \left(\frac{a_m m! \Delta_z^{m-n}}{(m-n)!n!} \right)$$
$$= \Sigma_{m=n+1} \left(\frac{m! p_m \epsilon^{m-n}}{(m-n)!n!} \right) \quad (15)$$

For the storage ring corrector magnets, at $|r| = 3$ cm, $p_n \leq 0.01$ for $n = 1,2,3$, $p_n \leq 0.03$ for $n = 4,5,6$ and $p_n \simeq 0$ for $n > 6$. Thus if $f_n = 0.2\%$ for $n = 1,2,3$, allowable $\epsilon_{max} = 0.016 \Longrightarrow \Delta_z \leq 0.048$ cm (0.019"), at which coil misalignment-induced sQ, sS, and sO are 0.03%, 0.05%, and 0.20% of sD, respectively. If we choose $f_n = 0.12\%$ for $n = 1,2,3$ allowable $\epsilon_{max} = 0.016 \Longrightarrow \Delta_z \leq 0.030$ cm (0.012"), at which coil misalignment-induced sQ, sS, and sO are 0.02%, 0.03%, and 0.12% of sD, respectively.

REFERENCES

[1] Jackson, A., *Magnetic Field Tolerances in the ALS Storage Ring*, LBL ESG Tech Note-103, Jan. 1989.

[2] Milburn, J., unpublished.

[3] Schlueter, R.D., Report LBL-32028, Lawrence Berkeley Laboratory, January 1991.

LAWRENCE BERKELEY LABORATORY
UNIVERSITY OF CALIFORNIA
TECHNICAL INFORMATION DEPARTMENT
BERKELEY, CALIFORNIA 94720